THE SOUTH POLAR HOT SPOT ON ENCELADUS. J. R. Spencer[1] J. C. Pearl, M. Segura, F. M. Flasar, A. Mamoutkine, and P. Romani[2], [1]Southwest Research Institute, 1050 Walnut St., Suite 400, Boulder, CO 80302, spencer@boulder.swri.edu, [2]NASA's Goddard Spaceflight Center, Greenbelt, MD 20771.

Summary: On July 14th 2005, Cassini's Composite Infrared Spectrometer (CIRS) detected 3 – 7 GW of thermal emission emanating from the "tiger stripe" troughs in the south polar region of Enceladus, at temperatures up to 145 K or higher. These warm troughs are presumably the source of the plume seen by multiple Cassini instruments. If the plume is generated by sublimation of H_2O ice, or the plume is in vapor pressure equilibrium with ice near the vent, and the sublimation source is visible to CIRS, vent temperatures of at least 180 K are required.

Global Thermal Properties: The first close Cassini flybys of Enceladus, on orbit 3 on February 17th 2005 and on orbit 4 on March 9th 2005, yielded 20 – 500 µm maps of Enceladus' low-latitude thermal emission, showing a diurnal brightness temperature range from ~55 K to ~75 K. Day and night temperatures near longitude 180 W can be matched by models with variable thermal inertias in the range 12 – 25 J m^{-2} $s^{-1/2}$ K^{-1}, averaged over the uppermost ~1 cm of the surface layer, with a bolometric albedo of 0.81, consistent with Voyager data (1), implying a very porous surface.

South Polar Hot Spot: The third flyby, on orbit 11 on July 14th 2005, provided a good view of the south polar regions of Enceladus for the first time. CIRS global mid-IR temperature maps with a spatial resolution of 25 km show enhanced 12 – 16 µm thermal emission from the region south of latitude 65 S, with brightness temperatures reaching 85 K near the south pole. The region of elevated south polar temperatures corresponds closely to a geologically youthful region occupied by four prominent troughs (dubbed "tiger stripes") seen by the Cassini cameras (2).

The average 12 – 16 µm spectrum of the 37,000 km^2 region south of 65 S is not consistent with blackbody emission, but after subtraction of expected background emission the spectrum can be fit by a graybody of temperature 133 ± 12 K occupying a small fraction (340^{+320}_{-160} km^2) of the surface. The corresponding non-solar emitted power is 5.8 ± 1.9 GW if the albedo of the warm regions is typical of the rest of the surface. This power estimate is a lower limit for the global power generated by Enceladus, as it does not include the potential power contributions from the kinetic and latent heat of the south polar plume seen by other Cassini instruments (2,3,4), or any heat radiated at lower temperatures or radiated elsewhere on Enceladus. The average heat flow over the region south of 65 S is 0.25 W m^{-2}, compared to ~2.5 W m^{-2} for Io (5). The depth to melting, or to ice warm and ductile enough to transport heat by convection, assuming pure solid H_2O ice and an ice conductivity of 3 x 10^5 erg cm^{-1} s^{-1} K^{-1} at the mean temperature of 180 K (6), is then only 2.5 km if the heat is generated below this level. In the localized warmer regions the inferred ice thickness is much less: a 125 K surface temperature implies a local heat flow of 13 W m^{-2}, and solid H_2O ice will approach the melting temperature at a depth of only 40 m. It is perhaps more likely that the heat is transported to the surface by advection of warm vapor rather than by conduction.

High-Resolution Observations: Correlation with Surface Features: During the last 2.5 hours of the approach to Enceladus on July 14th, CIRS obtained scattered coverage with mid-IR spatial resolution as fine as a few kilometers. These higher resolution observations show that the thermal emission is highly localized and is associated with individual prominent "tiger stripe" troughs (2,7). In some cases the source of the thermal emission can be pinpointed because CIRS observations were obtained near-simultaneously with ISS camera exposures, and the ISS field of view includes the 1 x 10 pixel CIRS mid-IR field of view. The location of the thermal emission observations relative to the geological features can then be determined very precisely, confirming the association with the troughs (Figure 1). The shapes of the hottest individual high resolution spectra, if interpreted as black bodies occupying a small fraction of the field of view, imply temperatures of at least 145 K

Lack of a North Polar Hot Spot: CIRS observed the north pole of Enceladus after closest approach, and we can rule out a northern hot spot similar to the southern one. A 20 – 500 µm integration of a 80 km diameter region centered on the north pole, which has been in darkness since 1995, determined a best-fit temperature of 32.9 ± 1.2 K, though this should perhaps be considered an upper limit because of the possibility that scattered radiation from surrounding warmer regions contaminated the signal. The corresponding thermal inertia, averaged over the penetration depth of the seasonal thermal wave (about 1 meter), is < 100 J m^{-2} $s^{-1/2}$ K^{-1}. Any north polar hot component at the temperature of the south polar spot (133 K) would have to have less than 15% of the heat flow of the south polar spot in order to avoid detection in this integration.

Plume Generation: It is likely that the warm south polar "tiger stripe" troughs are the source of the plume seen by other Cassini instruments (e.g. 2,3,4). From a stellar occultation measurement, the Cassini Ultraviolet Imaging Spectrometer (UVIS) detected a vapor plume above the south polar region (3), and determined an escape rate of 5 – 10 x 10^{27} molecules/sec. If we assume that the immediate origin of this plume is thermal sublimation of warm water ice (or equivalently, that the plume is in vapor pressure equilibrium with surface ice at its source), and that this warm ice is visible to the CIRS instrument (and is not, for instance, hidden in deep fractures), we can constrain the temperature of the plume source using the observed thermal emission from the south pole. The mean south polar radiance radiance at 900 cm^{-1}, about 5 x 10^{-10} W cm^{-2} str^{-1} $(cm^{-1})^{-1}$, places an upper limit on the exposed area of a high-temperature plume source at a given temperature, and thus, using the vapor pressure curve for water ice (8), an upper limit to the sublimation rate from this source. The UVIS escape rate can be reconciled with the observed 900 cm^{-1} radiance only for plume source temperatures of 180 K or higher. To produce the UVIS lower limit H_2O flux, a 180 K plume source would have an area of 28 km^2, equivalent for instance to a 55 meter width along 500 km of fractures. This compares to a ~700 meter width of material at 133 K along the same length of fractures (equivalent to the 340 km^2 area given above) required to explain the south polar thermal emission signature: there is likely a steep temperature gradient away from the tiger stripes.

Heat Source: An endogenic heat source is the most plausible explanation for these high temperatures, though solid-state greenhouse effects cannot be completely ruled out. Maximum available power from radiogenic heat, assuming a chondritic composition for the non-ice material in Enceladus, is about 0.1 GW (10), much smaller than observed. Tidal heating is a plausible alternate heat source: the orbital eccentricity of Enceladus, (0.0045, comparable to that of Io) is perhaps sufficient for significant tidal heating given the right internal structure and composition (11,12,13). However the absence of internal activity on nearby Mimas, which has an orbital eccentricity of 0.020, must then be addressed. The contrast with Mimas might be explained if Mimas is in a cold, elastic, non-dissipative state while Enceladus is in a self-maintaining warm, plastic, dissipative state (14). Resonantly-excited rotational librations have recently been suggested as a possible alternative tidal heating mechanism on Enceladus (15).

It is also possible that Enceladus is in an oscillatory state, as has been proposed for Io and Europa (16). In that case, its eccentricity and tidal heating rate may have recently been much higher, and perhaps the moon is still cooling down from that period.

References: [1] Hanel, R. *et al*., (1982), *Science* **215**, 544. [2] Johnson, T.V. et al. (2005), *AGU Fall 2005 meeting,* abstract #P21F-03. [3] Hansen, C.J. et al. (2005), *AGU Fall 2005 meeting,* abstract #P21F-04. [4] Dougherty, M.K., F.M. Neubauer, K.K. Khurana, and J. Saur (2005), *AGU Fall 2005 meeting,* abstract #P32A-02. [5] A.S. McEwen, L. P. Keszthelyi, R. Lopes, P. M. Schenk, J. R. Spencer (2004), in *Jupiter, the Planet, Satellites, and Magnetosphere*, F. Bagenal, T. Dowling, W. McKinnon, Eds. (U. Cambridge Press, Cambridge, UK), pp 307-328. [6] J. R. Spencer *et al.* (1997) in *Pluto and Charon*, S. A. Stern, D. Tholen, Eds. (U. Arizona Press, Tucson, AZ), pp 435-473. [7] Spencer, J.R. et al., *Science*, in press. [8] Bryson, C. E., V. Cazcarra, L. L. Levenson (1974) *J. Chem. Eng. Dat.* **19**, 107-110. [9] Squyres, S.W., R. T. Reynolds, P. M. Cassen (1983), *Icarus* **53**, 319. [10] Schubert, G., T. Spohn, R. T. Reynolds (1986), in *Satellites*, J. Burns, M. Matthews, Eds. (U. Arizona Press, Tucson, AZ), pp. 224-292. [11] Ross M.N. G. Schubert (1989), *Icarus* **78**, 90. [12] S. W. Squyres, R. T. Reynolds, P. M. Cassen (1983), *Icarus* **53**, 319. [13] Czechowski, L, (2004) paper presented at the 35th COSPAR Scientific Assembly, Paris, France. [14] Czechowski, L., L J. Leliwa-Kopystyński, (2005) *Planet. Space Sci.* **53**, 749. [15] Wisdom, J. (2004), *Astron. J.* **128**, 484. [16] Hussmann, H., T. Spohn (2004), *Icarus* **171**, 391.

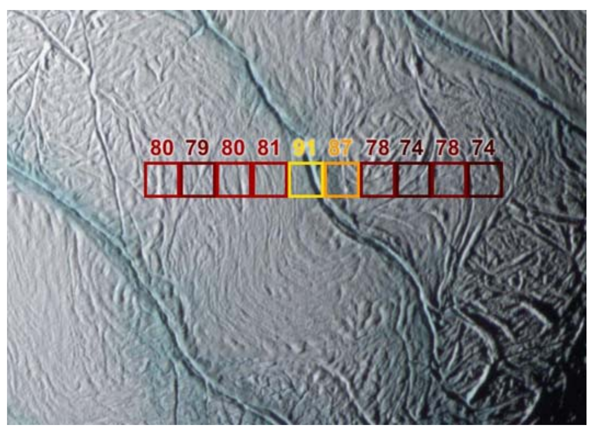

Figure 1 Correlation of warm CIRS 12 – 16 µm brightness temperatures, in Kelvin (color coded numbers), with the "tiger stripe" fractures seen by the ISS cameras in the south polar region of Enceladus. Each square CIRS field of view is 6 km across. Cassini CIRS/ISS press release image PIA06433.